Determination of active sites during gasification of biomass char with CO_2 using temperature-programmed desorption. Part 1: Methodology & desorption spectra

Christoph Schneider[a,*], Sonia Rincón Prat[b], Thomas Kolb[a,c]

[a] *Karlsruhe Institute of Technology, Engler-Bunte-Institute, Fuel Technology, EBI-ceb, Engler-Bunte-Ring 1, 76131 Karlsruhe, Germany*
[b] *Universidad Nacional de Colombia, Departamento de Ingeniería Mecánica y Mecatrónica, Grupo de Investigación en Biomasa y Optimización Térmica de Procesos, BIOT, Carrera 30 No 45A-03, Bogotá, Colombia*
[c] *Karlsruhe Institute of Technology, Institute for Technical Chemistry, ITC-vgt, Hermann-von-Helmholtz-Platz 1, 76344 Eggenstein-Leopoldshafen, Germany*

Keywords:
Biomass char
Gasification kinetics
Surface chemistry
Temperature-programmed desorption
Active sites

A B S T R A C T

Based on a carbon conversion mechanism for the gasification of carbon with CO_2, a method for the determination of active sites during gasification of biomass char is presented. Beech wood char was partially gasified in CO_2 followed by a temperature-programmed desorption (TPD) in order to determine total and stable surface complexes as a function of carbon conversion degree. The experiments were conducted in a temperature controlled quartz glass reactor coupled with a mass spectrometer for the detection of desorbed gas species (CO and CO_2). Similar CO_2 signals for total and stable surface complexes are observed for all carbon conversion degrees. Increased release of CO during the determination of total and stable surface complexes is detected for $X_C = 0.9$ carbon conversion degree. The desorption spectra of CO and CO_2 during TPD cannot completely be explained by the underlying mechanistic model. The measured concentration profiles indicate that the gas species released during TPD may originate from decomposition of surface complexes but also from decomposition of ash components. CO and CO_2 arising from of ash components or surface complexes must be differentiated in order to determine reactive surface area (RSA) as a function of carbon conversion degree which is then transferred into a kinetic rate expression for the specific conversion rate R_m. This paper describes the methodology applied for the determination of RSA and discusses the raw data obtained during TPD. In part 2, a detailed analysis concerning the origin of the released gases during TPD is conducted.

1. Introduction

The biomass gasification process has gained wide attention following the discussion on utilization of renewable sources for production of chemicals and the supply of power and heat. The syngas from entrained flow gasification of biogenic residues is suitable for the production of a wide variety of liquid fuels (gasoline, diesel), gaseous fuels (synthetic natural gas) and chemicals (methanol, dimethyl-ether – DME, ethanol, ammonia), as well as electric power (gas turbines and integrated gasification combined cycle plants) [1]. The present work is part of the research activities of the BtL bioliq® project which includes a gasification step in a 5 MW_{th} input high-pressure oxygen-blown entrained flow gasifier (EFG). As feedstock for the gasifier, a suspension fuel (slurry) based on pyrolysis oil and char, produced from biogenic residues (e.g. straw) in a fast pyrolysis process is used. [2]. The slurry is fed to the gasifier via a burner, inside the reactor the liquid phase of the slurry droplets evaporates rapidly. Subsequently, the char is heated up and undergoes a secondary pyrolysis process characterized by high heating rates. Downstream of the gasifier flame zone the secondary char reacts with H_2O and CO_2 to the final syngas. As the heterogeneous secondary char gasification is the rate-determining step of the gasification process, understanding the complex physical and chemical processes that take place during the gasification reactions has been identified as one of the knowledge gaps that restrict mathematical modelling and design of technical entrained flow gasifiers.

2. Literature review

The heterogeneous gasification of char particles is controlled by process parameters, i.e. temperature, partial pressure of the reactant gas and process pressure as well as the chemical and physical properties of the char. Char properties change as char conversion proceeds, which

* Corresponding author.
E-mail addresses: ch.schneider@kit.edu (C. Schneider), slrinconp@unal.edu.co (S. Rincón Prat), thomas.kolb@kit.edu (T. Kolb).

in turn causes changes in char conversion rate with progressing conversion degree. Although the properties of biomass chars have been studied extensively [3], less attention has been paid to the fundamental understanding of the reaction mechanisms and the role of the variable chemical and physical properties of the char during the gasification process. The relevant physical properties are total internal surface area, porosity, pore size distribution and char carbonaceous structure and ordering [4]. Chemical properties of char affecting conversion rate are related to active sites and functional groups available at the char surface as well as to the presence of catalytic minerals embedded as ash in the char particle.

The oxygen exchange mechanism presented in R1 to R3 [5] is widely accepted as reaction mechanism describing the carbon/char gasification with CO_2.

$$C_f + CO_2 \xrightarrow{k_1} C(O) + CO \quad (R1)$$

$$C(O) + CO \xrightarrow{k_2} C_f + CO_2 \quad (R2)$$

$$C(O) \xrightarrow{k_3} CO \quad (R3)$$

C_f represents an active site on the char surface and C(O) a carbon-oxygen intermediate, respectively. Assuming first-order dependency on carbon concentration and pseudo zero-order dependency on gas concentration, the specific conversion rate R_m can be written according to the fundamental kinetic expression [6]

$$R_m = -\frac{1}{m_C(t)}\frac{dm_c}{dt} = \frac{1}{1 - X_C(t)}\frac{dX_C}{dt} = kC_{C_f} \quad (1)$$

where C_{C_f} is the surface concentration of active sites available for the reaction, X_C the carbon conversion degree and $\frac{dX_C}{dt}$ the carbon conversion rate. For modeling of the char gasification process, the concentration of carbon active sites has to be determined as a function of carbon conversion degree. The carbon conversion degree can be expressed by a mass balance with $m_C(t)$ as the time dependent and $m_{C,0}$ as the initial carbon mass:

$$X_C(t) = \frac{m_{C,0} - m_C(t)}{m_{C,0}} \quad (2)$$

Wölki [7] presented a detailed summary of kinetic expressions for biomass char gasification with H_2O and CO_2 under atmospheric pressure. These expressions do not take into account the evolution of chemical or physical properties of chars during gasification reaction. Thus, they are only valid for a certain carbon conversion degree range [3,8]. Other authors have included a term that accounts for changes in physical properties in the kinetic equations. In a review on combustion and gasification rates of ligno cellulosic chars, Di Blasi [3] presented expressions that include a structural term which depends exclusively on char conversion degree. More complex particle models account for the variation of physical properties of the char during gasification in terms of porosity, pore diameter and length as well as total surface area. Lizzio et al. [9] give a summary of five coal gasification models that include general expressions for the variation of structural parameters e.g. the random pore model (RPM) of Bathia and Perlmutter [10] describing growth and collapse of the pore structure of a char particle during conversion. Regarding biomass char gasification, Gómez-Barea and Leckner [11] present a summary of existing structural models. The RPM and its modifications (MRPM) have been successfully used in some cases concerning biomass char gasification [12–16]. Moreover, Fatehi and Bai [17] as well as Singer and Ghoniem [18] propose models describing the evolution of a multimodal pore structure. Experimental values for the variation of structural properties i.e. specific surface area, pore size distribution and porosity of biomass char during gasification can be found in literature [4,19–21]. Although these structural models describe the evolution of carbon conversion and conversion rate, their application is restricted as the model parameters are very difficult to be determined experimentally.

Studies on the reaction kinetics of biomass char gasification addressing the influence of chemical properties use the theory of active sites developed in the working group of Walker. The approach was presented originally by Laine et al. [22] in 1963 and further developed until the early nineties [6,9,23]. The theory is based on the mechanistic understanding of catalytic heterogeneous reactions where the catalytic activity is proportional to the active surface area (ASA) of the catalyst. As presented in reactions R1 to R3, gasification proceeds via oxygenated surface complexes, so-called carbon-oxygen intermediates (C(O)). Thus, the quantity of these complexes available for the reaction is a direct measure of the specific conversion rate. A first approximation of the quantification of the surface area available for the reaction is the utilization of the total accessible surface area (TSA) determined by physical adsorption and applying the Brunauer-Emmett-Teller (BET) [24] or Dubinin-Radushkevich (DR) [25] models. The evolution of TSA during char gasification can be predicted by the models mentioned above. These approaches assume either that the gasification reactions occur everywhere on the char surface (TSA) or that there is a linear relationship between ASA and TSA. However, this model concept is not able to explain the correlation between char surface and conversion rate, since chars of similar TSA can show significantly different conversion rates and a linear relationship between conversion rate and TSA has not been reported [4,6,20,22].

The quantification of the surface area available for the reaction can be accomplished by measurement of the amount of oxygenated surface complexes formed during gasification by the temperature-programmed desorption technique. Oxygenated surface complexes are bound on the surface of carbonaceous materials in the form of oxygen functional groups, such as lactones, carbonyls, anhydrides, phenols, ethers and quinones. During desorption, the bonds of these functional groups are destroyed resulting in the release of the gaseous species such as CO, CO_2 and H_2O [26–30].

Laine et al. [22] proposed an approach based on their research on the carbon – oxygen reaction of highly purified graphitized carbon black. They determined the active surface area from the quantity of surface complexes formed on in situ partially oxidized samples through chemisorption experiments with oxygen at 300 °C followed by a desorption *in vacuo* up to 950 °C. They define the unoccupied active surface area (UASA), which corresponds to the term reactive surface area used later in the present work, as the quantity of active sites at which the reaction occurs and no formation of stable complexes takes place. Stable complexes are defined as being formed during reaction remaining on the surface at reaction conditions i.e. blocking active sites for further reaction. Wölki [7] presents a summary of numerous investigations that followed the procedure proposed by Laine et al. [22] for the measurement of ASA on chars using O_2, CO_2 and H_2O as reactive gases. Although in these investigations no linear relationship between specific conversion rate and experimentally determined ASA was found, it could be concluded that ASA depends on temperature and partial pressure of the reactive gas. The value of ASA is only a small fraction of the total surface area (TSA). These findings reveal that a suitable approach for the experimental determination of available active sites during char conversion is the UASA and not the ASA from low temperature chemisorption [9,31]. 23 years after Laine et al. [10], Lizzio et al. [9] introduced the concept of reactive surface area (RSA) as a measure for active sites that are capable to chemisorb the reactant gas dissociatively but do not form a stable complex (C-O). These authors add an extra step (R4 and R5) to the oxygen exchange mechanism presented before accounting for the formation of a stable C-O complex from a carbon–oxygen intermediate during gasification.

$$C_f + CO_2 \xrightarrow{k_1} C(O) + CO \quad (R1)$$

$$C(O) + CO \xrightarrow{k_2} C_f + CO_2 \quad (R2)$$

$$C(O) \overset{k_4}{\rightarrow} C\text{-}O \quad \text{(R4)}$$

$$C\text{-}O \overset{k_5}{\rightarrow} C(O) \quad \text{(R5)}$$

$$C\text{-}C(O) \overset{k_6}{\rightarrow} CO + C_f \quad \text{(R3*)}$$

The carbon–oxygen intermediate C(O) desorbs either as CO (R3*), leaving a new active carbon site C_f or forms a stable complex C–O (R4). This mechanism is based on the assumption that reactions R4 and R5 are in equilibrium at constant temperature. Furthermore, it is assumed that stable complexes C-O cannot be desorbed. Accounting for a closed carbon balance, the reaction R3* has been slightly modified as compared to literature. R3* produces a new carbon active site as long as excess carbon is available [9].

The determination of RSA requires experiments at reaction temperature either using temperature programmed desorption (TPD) or transient kinetics (TK) [7,9]. The method of transient kinetics proposed by Freund [32] for the study of desorption of oxygen surface complexes allows a direct determination of RSA. After gasification to a desired carbon conversion degree, the flow of reacting gas is changed to inert gas and the desorption of oxygen containing gases is continuously recorded. The quantity of desorbed gases corresponds to the number of reactive sites available at the experimental conditions chosen. The suitability of the method was intensively studied and proven by Radovic et al. [9,33,34]. The method was also applied by other authors concerning the study of gasification reactions of coal chars [35,36]. The TPD method was successfully used by several authors for the determination of surface complexes of partially gasified char samples [8,9,37–39]. RSA is determined indirectly based on a two-step procedure proposed by Lizzio et al. [9]. In a first experiment (procedure 1), a partially gasified sample is quenched in reactant gas. As the activation energies for adsorption and migration of oxygen species are lower than the activation energy for desorption, the desorbed unstable C(O) complexes are quickly replaced by new C(O) complexes in the presence of excess CO_2 during the quench procedure [40]. Thus, all carbon oxygen intermediates (stable C-O and unstable C(O) complexes) are preserved. In a second experiment (procedure 2) using the same gasification conditions, the flow of reactant gas is switched to inert gas at reaction temperature. In this case, unstable C(O) complexes desorb while stable C-O complexes remain on the char surface. The quantification of total surface complexes (TSC) (procedure 1) and stable complexes (procedure 2) is accomplished by submitting the samples to temperature-programmed desorption, measuring the amount of released oxygen-containing gases. RSA is calculated as the difference between total and stable surface complexes. A detailed description of the experimental procedure is given in chapter 3.

Research that concentrates on the measurement of the formation of active sites during gasification of biomass char is rare. Klose & Wölki [8] presented experimental results in 2005 on the quantification of RSA using the TPD procedure for the gasification of beech wood char and oil palm shell char with CO_2 and H_2O. They determined kinetic parameters for the intrinsic reaction rate using a Langmuir-Hinshelwood type rate expression and found a linear relationship between the measured RSA and the reaction rate. Zoulalian et al. [41] developed a mathematical model that accounts for the evolution of RSA with increasing carbon conversion degree. The theoretical results are in good agreement with the experimental work presented by Lizzio et al. [9] and Klose & Wölki [8]. Guizani et al. [4] studied variations in chemical and physical properties of beech wood char during gasification with CO_2, H_2O and its mixtures. They conducted TPD experiments of partially gasified samples, where the flow of reactive gas was switched to nitrogen and quickly cooled down after reaching the desired conversion degree. Interpreting the concentration over temperature profiles of the released gas species, they qualitatively determined possible oxygenated functional groups present in the samples based on literature data.

In order to further improve the fundamental understanding of phenomenological changes during char gasification, in this work, an experimental method for quantification of total, stable and unstable complexes during gasification of a biomass char based on the method proposed by Lizzio et al. [9] and Klose & Wölki [8] is applied. However, special focus is put on the interpretation of the gas species profiles in order to determine the contributions of desorption of oxygenated surface complexes and possible influence of ash decomposition reactions during TPD. The validity of the mechanism based on Lizzio et al. [9] is applied to describe the gasification process of a biomass char pyrolyzed in a drop-tube reactor. The experimental determination of total surface complexes (TSC), stable complexes (C-O in equilibrium with C(O) in R4 and 5) and unstable complexes (C(O) leading to the formation and desorption of gaseous CO in R3*) is presented.

$$C_f + CO_2 \overset{k_{1,2}}{\leftrightarrow} C(O) + CO \quad \text{(R1-R2)}$$

$$C(O) \overset{k_{4,5}}{\leftrightarrow} C\text{-}O \quad \text{(R4-R5)}$$

$$C\text{-}C(O) \overset{k_6}{\rightarrow} CO + C_f \quad \text{(R3*)}$$

3. Materials and methods

3.1. Biomass char characterization

The biomass char used in this study was produced from a bark-less beech wood. Wood chips were chopped and fed to a screw-pyrolysis reactor which is described elsewhere [42,43]. The primary pyrolysis was conducted at 500 °C at a residence time of five minutes for the solid material. The resulting char was milled and sieved to particle sizes in the range of 50 to 150 μm. The char underwent a secondary pyrolysis in a drop-tube reactor at 1600 °C in order to produce a char with low volatile content under high heating rates and short residence time (200 ms), i.e. the char was produced under typical conditions of entrained-flow gasification (EFG). The char (WC1600) [44] was sieved to a 50–100 μm fraction. Physical and chemical data of the biomass char can be found in Table 1.

3.2. Experimental set-up

Experiments in terms of partial gasification and temperature-programmed desorption (TPD) at atmospheric pressure were carried out in

Table 1
Properties of WC1600.

Proximate analysis/wt.-%, ad	
Moisture	1.1
Ash content	6.6
Volatiles	4.6
Fixed carbon	87.7
Ultimate analysis/wt.-%, daf	
C	97.4
H	< 0.1
O (diff)	1.6
N	1.0
Ash composition analysis/wt.-%	
Na_2O	0.5
K_2O	9.1
MgO	1.6
CaO	30.1
Fe_2O_3	2.6
Al_2O_3	3.5
SiO_2	25.8
Structural parameters	
Specific Surface Area/$m^2\ g^{-1}$	62.1
Skeletal density/g cm^{-3}	2.0
Hg intrusion porosity/%	83.4

a chemisorption analyzer (MicrotracBEL, BELCAT-II). A schematic drawing of the reactor system is given in the supplementary material section. The reactor consists of two concentric quartz glass tubes. The reactant gas is introduced through the outer tube to be heated up to reaction temperature. The char sample is positioned between two quartz wool layers in the inner tube of the reactor (inner diameter d = 8 mm). The sample temperature is monitored by a type K thermocouple. Gas species (CO, CO_2, Ar) are continuously analyzed by a quadrupole mass spectrometer (MS) (IPI, GAM 400). The char sample is quenched by cooling the external surface of the outer reactor tube with air at ambient temperature.

3.3. Experimental procedure

Raw biomass char was gasified up to conversion degrees *X*c of 0.25, 0.50, 0.75 and 0.90. Prior to each gasification procedure, the char sample was degassed for 1 h at 900 °C in flowing Ar and cooled down to gasification temperature. In the next step, partial gasification up to the desired carbon conversion degree at 820 °C and atmospheric pressure in 80 vol–% CO_2 and 20 vol-% Ar was conducted. A sample mass of 30 mg and a total volume gas flow of $\dot{V}_{in,STP}$ = 100 ml min^{-1} were applied in order to avoid transport limitations. With these process parameters, a maximum reduction of CO_2 concentration due to reaction below 3 vol-% was assured, i.e. the chemisorption analyzer was operated as differential reactor.

For the determination of total surface complexes (TSC), the sample was quenched to 200 °C in reactant gas atmosphere. After the CO concentration detected in the off-gas reached baseline level, i.e. no more gasification took place, the gas atmosphere was switched to Ar. Subsequently, a TPD was performed in flowing Ar ($\dot{V}_{STP}$= 50 ml min^{-1}) with a heating rate of 3 K/min to a final temperature of 900 °C. This temperature was kept constant for 1 h to achieve complete desorption of surface complexes. Volume fractions of CO and CO_2 ($y_{CO,total}$ and $y_{CO_2,total}$) were measured in the off-gas and plotted over time (see Fig. 3).

For the determination of stable C-O complexes, the experimental procedure was modified. After gasifying the char to the desired carbon conversion degree, the gas atmosphere was switched to Ar at reaction temperature in order to desorb all unstable C(O) complexes. After the CO and CO_2 concentrations reached zero level, the char sample was quenched in flowing Argon to 200 °C. Again, a TPD was performed as described previously and volume fractions of CO and CO_2 ($y_{CO,stable}$ and $y_{CO_2,stable}$) were measured (see Fig. 3).

In both experimental procedures, quenching from 820 °C to 400 °C was achieved within 5 min. The time required for the additional cooling to 200 °C was 7 min. In order to set a base line for the CO and CO_2 signals, blank experiments without char sample using only Ar as carrier gas were performed following the same heating program as the one for the determination of total surface complexes. Here, no CO_2 signal was observed, the CO signal, however, showed a continuous increase beginning at approx. 450 °C up to 0,003 vol-% at 900 °C. This baseline signal was subtracted from all CO signals obtained.

3.4. Data analysis

3.4.1. Gas phase analysis

Calibration of the MS was carried out for CO, CO_2 and Ar before and after each experiment. Mass flow controllers of the chemisorption analyzer were also checked versus a volumetric flowmeter (Ellutia, 7000 GC Flowmeter). The following equations were used to assign ion currents of a certain mass-to-charge ratio to the corresponding gas volume fractions of Ar and CO_2 [45]:

$$I_{40}(t) = S_{Ar} p_{total} y_{Ar}(t) \tag{3}$$

$$I_{44}(t) = S_{CO_2} p_{total} y_{CO_2}(t) \tag{4}$$

Here, $I_{m/z}$ is the ion current of a certain mass-to-charge ratio (m/z), S_i is the sensitivity of the gas species i, p_{total} is the total pressure (1 bar) and y_i is the volume fraction of the gas species i. Difficulties in the determination of the CO concentration arise from fragmentation of CO_2. This effect needs to be taken into account by a relative intensity a_{28} at a mass-to-charge ratio of 28:

$$a_{28} = \frac{I_{28}}{I_{44}} \tag{5}$$

$$I_{28}(t) = S_{CO_2} a_{28} p_{total} y_{CO_2}(t) + S_{CO} p_{total} y_{CO}(t) \tag{6}$$

Experimental values for a_{28} in the range of 0.090–0.095 are in good agreement with literature [46]. Sensitivities S_i and relative intensity a_{28} were determined for each experiment. Calibrations were carried out with 3 vol-% CO, 5 vol-% CO_2 and 80 vol-% CO_2 in Argon.

3.4.2. Calculation of carbon conversion degree

Considering only the Boudouard Reaction, the carbon conversion degree X_C can be calculated by a carbon balance according to following equations (Eqs. 7–10):

$$\frac{dX_C}{dt} = \frac{y_{CO}(t)}{2} \frac{M_C}{m_C} \dot{n}_{out}(t) \tag{7}$$

$$\dot{n}_{out}(t) = (\dot{n}_{Ar,in} + \dot{n}_{CO_2,in}) \frac{1}{1 - 0.5 y_{CO,out}(t)} \tag{8}$$

M_C represents the molar mass of carbon, m_C the converted mass of carbon which was calculated from the CO signal in the exhaust gas by a carbon balance (Eq. 7) and $\dot{n}_{out}$ the molar gas flow of the exhaust gas which can be calculated from the inlet gas flows of Ar and CO_2 and the measured CO concentration in the off-gas. The converted mass of carbon m_C can be calculated as:

$$m_C = \frac{M_C}{2} \int_0^{t_{end}} y_{CO}(t) \dot{n}_{out}(t) dt \tag{9}$$

Finally, the time dependent carbon conversion degree $X_C(t)$ is calculated by:

$$X_C(t) = \frac{\int_0^t y_{CO}(t) \dot{n}_{out}(t) dt}{\int_0^{t_{end}} y_{CO}(t) \dot{n}_{out}(t) dt} \tag{10}$$

Specific conversion rate R_m as a function of carbon conversion degree is calculated according to Eq. 1.

3.4.3. Analysis of released CO and CO_2 signals during TPD

Molar flows of CO_2 and CO during TPD are determined according to Eq. 11 with i being either CO or CO_2. This equation takes into account the increment in the gas flow due to the released gas during TPD. The amount of desorbed gas species n_{CO} and $n_{CO_2}$is determined by integration of Eq. 11 (see Eq. 12).

$$\dot{n}_i(t) = y_i(t) \left(1 + \frac{y_{CO_2}(t)}{y_{Ar}(t)} + \frac{y_{CO}(t)}{y_{Ar}(t)}\right) \frac{p_{STP} \dot{V}_{Ar}}{R T_{STP}} \tag{11}$$

$$n_i = \int_0^{t_{end}} \dot{n}_i(t) dt \tag{12}$$

The total quantity of active sites where surface complexes are formed is calculated assuming that one surface complex contains one oxygen atom. The number of complexes is determined by summing up the amount of oxygen atoms released in CO and CO_2 during TPD. This approach is valid for total, stable and unstable complexes using the corresponding CO and CO_2 signals. In the present work, the mass specific quantity of reactive sites $x_{reactive}$ is expressed as the mass fraction of carbon atoms on which surface complexes participating in the gasification reaction are formed (C_f) divided by the actual mass of carbon according to the following expression [22].

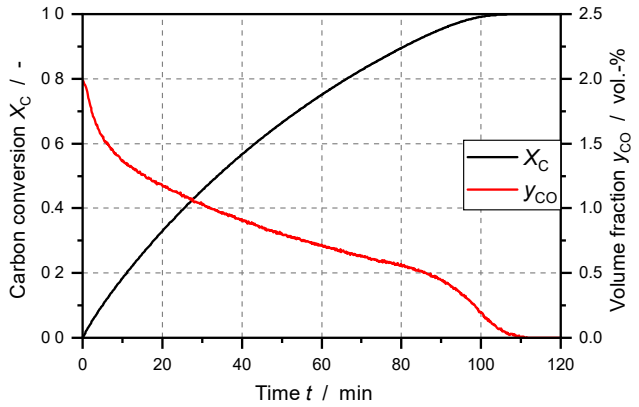

Fig. 1. Carbon conversion and CO volume fraction as a function of time; gasification of WC1600 at 820 °C with 80 vol-% CO_2 and 20 vol-% Ar at atmospheric pressure in the chemisorption analyzer.

$$x_{\text{reactive}} = \left[(n_{\text{CO,total}} - n_{\text{CO,stable}}) + 2(n_{\text{CO}_2\text{,total}} - n_{\text{CO}_2\text{,stable}})\right] \frac{M_C}{m_{C,0}(1 - X_C)} \quad (13)$$

$m_{C,0}$ corresponds to the initial mass of unconverted carbon and X_C to the carbon conversion degree defined in Eq. 10. M_C is the molar mass of carbon.

4. Results and discussion

4.1. Gasification experiment

Fig. 1 shows an example of the experimentally obtained volume fraction of CO in the exhaust gas of the chemisorption analyzer and the calculated carbon conversion degree (Eq. 10) during complete gasification of WC1600 at 820 °C in a mixture of 80 vol-% CO_2 and 20 vol-% Ar. The CO concentration has a maximum value of 2 vol-% at the beginning of the gasification process and decreases steadily. At 90% conversion degree, a steep decrease in CO concentration is observed.

Fig. 2 shows the char conversion rate and the specific conversion rate (calculated according to Eqs. 7 and 1, respectively) as a function of carbon conversion degree for the experiment shown in Fig. 1. The conversion rate decreases steadily over the whole conversion process; in the range Xc = 0.15–0.9 the char conversion rate shows an almost linear decrease. For Xc = 0–0.15 and even more pronounced for Xc > 0.9, a steeper decrease is observed. Specific conversion rate R_m increases slowly until Xc = 0.6 carbon conversion degree is reached. From this point, R_m increases significantly as the remaining carbon

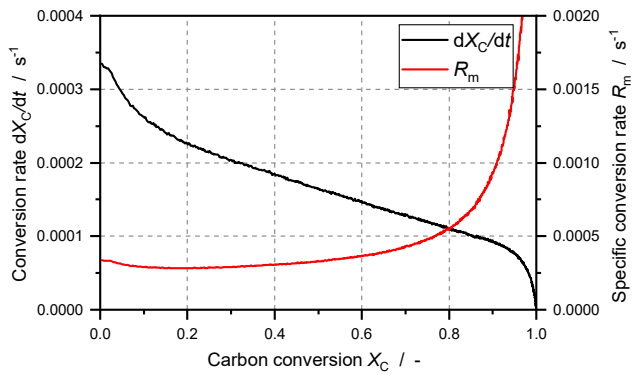

Fig. 2. Conversion rate and specific conversion rate as a function of carbon conversion; gasification of WC1600 at 820 °C with 80 vol-% CO_2 and 20 vol-% Ar at atmospheric pressure in the chemisorption analyzer.

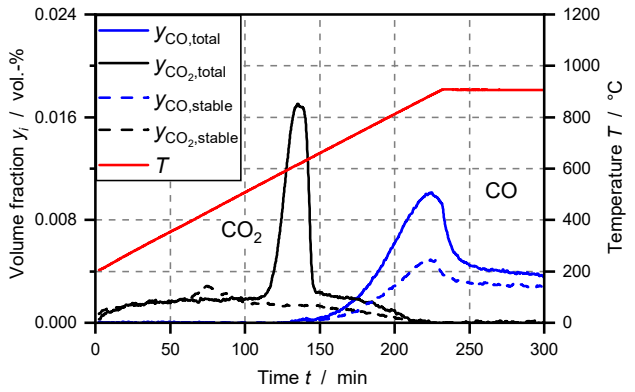

Fig. 3. TPD spectra for the WC1600 char samples gasified up to Xc = 0.75; gasification of WC1600 at 820 °C with 80 vol-% CO_2 and 20 vol-% Ar at atmospheric pressure in the chemisorption analyzer; total and stable complexes desorbed as CO_2 and CO.

mass approaches zero. Reported values for R_m and conversion rate are in the range of literature data [8].

4.2. Temperature-programmed desorption spectra

Fig. 3 shows the desorption spectra of CO and CO_2 for the detection of total and stable surface complexes exemplarily for Xc = 0.75 carbon conversion degree. Similar spectra are obtained for all experiments with different carbon conversion degrees.

As it is assumed by the reaction mechanism proposed by Lizzio et al. [9], total and stable surface complexes must originate from oxygenated carbon atoms on the char surface (also noted as carbon–oxygen intermediates). The release of CO_2 during TPD may arise from the decomposition of lactones between 190 °C and 650 °C [26]. During the TPD experiments carried out, CO_2 desorption starts at 200 °C and is observed over almost the whole temperature range investigated. At 850 °C, complete desorption of CO_2 is achieved. CO_2 shows a similar trend up to 380 °C for both TPD-procedures i.e. total and stable complexes. Above 380 °C, differences in total and stable CO_2 can be observed. Between 380 and 500 °C, the CO_2 signal of the stable complex curve is above the signal of the total complexes, showing a reproducible maximum at 430 °C. Regarding the mechanisms considered, total CO_2 has to be higher than stable CO_2. Extra CO_2 evolution must arise from other reactions where CO_2 is released during the desorption step in the experiments for determination of stable complexes.

Concerning the analysis of total surface complexes, a dominant CO_2 peak between 550 °C and 650 °C is observed. At higher temperatures, the CO_2 signal of the total complexes remains slightly higher than the one of the stable complexes. The difference in the signals may be attributed to the formation of oxygenated complexes on the char surface during gasification, which are released as CO_2.

Regarding the release of CO arising from oxygenated carbon complexes on the char surface, it may originate from the decomposition of carbonyls, ethers and quinones within a temperature range of 700 °C to 980 °C [26]. During the TPD experiments, the CO signal begins to increase at 600 °C with a maximum near 900 °C. CO signals of total and stable complexes show a similar course but with a higher value for the total surface complexes. In the isothermal part of the TPD at 900 °C the CO does not reach baseline level.

The experimental data reported in Fig. 3 some features that do not correspond to the underlying mechanistic model by Lizzio et al. [9]:

(i) CO_2 release around T = 430 °C implies higher amount of stable complexes than total complexes.
(ii) CO signal does not reach baseline line level in the isothermal part of the TPD at 900 °C.

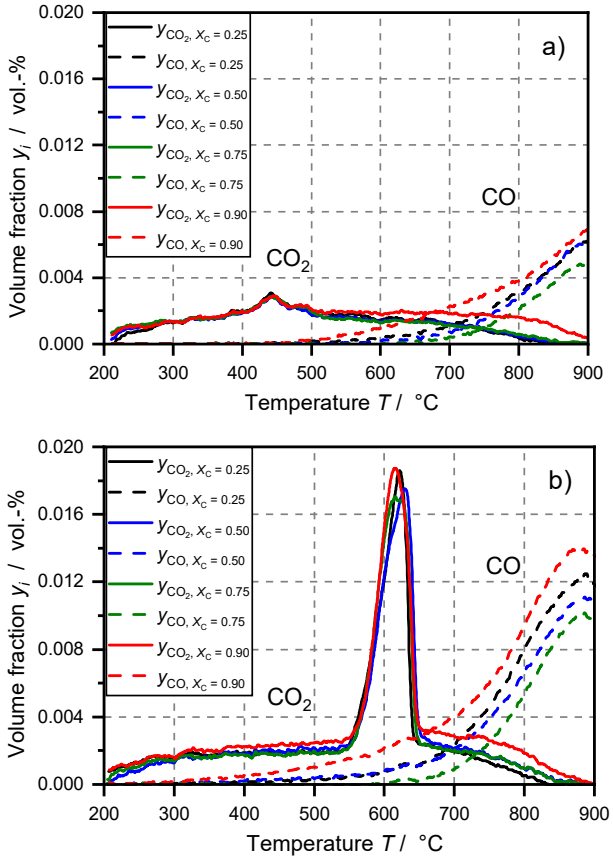

Fig. 4. TPD spectra of CO_2 and CO for the gasification of WC1600 as function of temperature with increasing carbon conversion for (a) stable surface complexes (b) total surface complexes. Gasification of WC1600 at 820 °C with 80 vol-% CO_2 and 20 vol-% Ar at atmospheric pressure in the chemisorption analyzer.

As all our experiments were reproduced, there is no evidence for experimental error. The deviations observed need considerations beyond the mechanistic models for the uncatalyzed heterogeneous char gasification reaction. Part 2 of our research report is focused on the explanation of these effects, which are due to:

(i) Decomposition processes of inherent ash components [47–50].
(ii) Desorption of chemisorbed CO_2 at low temperatures [51].
(iii) CO forming reactions from silica with carbon above 800 °C [52,53].

Basic experiments to show the influence of ash decomposition are given in Section 4.3 of this paper.

4.3. Effect of X_C on desorption spectra

Fig. 4 shows desorption spectra of CO and CO_2 during the determination of total and stable surface complexes for the four carbon conversion levels studied (Xc = 0.25, 0.50, 0.75 and 0.90) as a function of temperature.

The release of CO_2 from stable surface complexes (see Fig. 4 (a)) shows exactly the same profile for all conversion degrees. Only for 90% conversion degree, the high temperature section (650–900 °C) is slightly more pronounced.

The consistency in the profiles may be explained either by:

(i) The same amount of stable C-O complexes during gasification for all carbon conversion degrees observed.
(ii) No formation of stable complexes, CO_2 is released only by ash decomposed during TPD then the same CO_2-release profile irrespective of conversion degree would be expected. If the amount of ash remained constant during gasification, the same quantity must decompose during TPD.

The CO_2 signal of total complexes also shows a similar profile with a peak between 550 °C and 600 °C for all carbon conversion degrees (Fig. 4(b)). A difference can be observed for the sample with Xc = 0.9, where a slightly higher CO_2 signal is detected at T > 700 °C.

Regarding CO, the signals for both stable and total surface complexes decrease slightly from Xc = 0.25 to 0.75 followed by a steep increase for the Xc = 0.9 case. For both stable and total complexes, the signals of the chars at Xc = 0.25, 0.50 and 0.75 conversion have the same form while the signal of the sample for Xc = 0.90 shows an increased release of CO between 500 °C and 850 °C. Possible interpretations for the increased CO signal are:

(i) Enhanced formation of oxygenated surface complexes at Xc = 0.9.
(ii) Decomposition of potassium carbonates at temperatures higher than 700 °C mainly yielding CO [54,55].

In conclusion, CO and CO_2 released during TPD may arise from either desorption of oxygenated surface complexes or ash decomposition reactions. Total and stable complexes released as CO_2 follow the same trend for each conversion degree. Stable complexes show a reproducible peak at approx. 430 °C, which is higher than the CO_2 signal of the total surface complexes. Assuming that this peak cannot arise from desorption of surface complexes, it has to be the result of ash decomposition reactions favored by the experimental procedure applied for the determination of stable complexes. In order to clarify the observed effects, the influence of ash decomposition reactions on the detected signals was investigated by TPD experiments of samples, which were not subjected to gasification and with ash samples resulting from complete gasification of the char.

4.4. Desorption spectra of unconverted and completely gasified char sample

In order to evaluate the influence of ash decomposition reactions on the obtained desorption spectra blank experiments were performed where no surface complexes should have been formed. Here, the procedure for the determination of stable surface complexes was applied. The first experiment was conducted with WC1600 using the same heating program as for the determination of stable complexes but using Ar rather than CO_2 in the gasification segment i.e. there was no production or conversion of carbon-oxygen intermediates. In the second experiment, a complete conversion of the char sample was first carried out in a CO_2 atmosphere. Both sample underwent the standard TPD procedure for stable complex detection, i.e. Ar quench and desorption. The obtained desorption spectra are shown in Fig. 5. For comparison, the desorption spectra of the determination of stable complexes at X_C = 0.25 conversion degree is included in Fig. 5.

The CO_2 signal (see Fig. 5(a)) shows the highest intensity for the unconverted char and decreases with conversion degree. As the unconverted char was not subjected to CO_2 and potential surface complexes must have been desorbed in the heating pretreatment under Ar atmosphere prior to TPD, the CO_2 release cannot arise from the desorption of stable complexes. This result indicates that part of the CO_2 release of the samples submitted to gasification originates from decomposition reactions of ash components inherent in the char. The decrease of the CO_2 signals for increasing carbon conversions may be the result of sintering processes of Ca particles leading to a lower Ca dispersion [56]. Thus, a lower amount of carbon in the immediate vicinity of the Ca particles can react to form $CaCO_3$, which then decomposes during TPD releasing CO_2.

Furthermore, the CO_2 signal of the unconverted char (X_C = 0) shows a different course as compared to the samples gasified up to

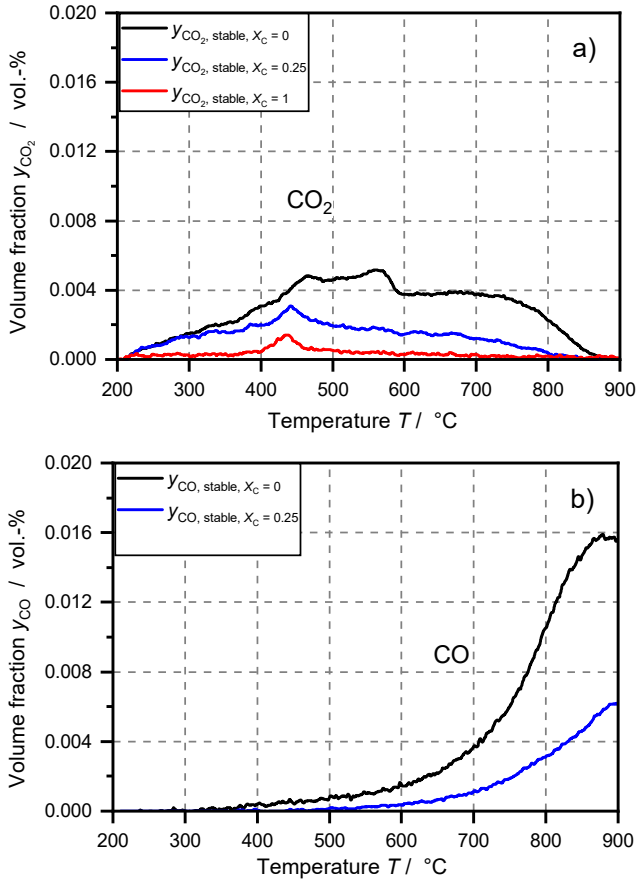

Fig. 5. TPD spectra for the determination of stable complexes of WC1600 for carbon conversion degrees of (a) $Xc = 0/0.25/1$ for CO_2 and (b) $Xc = 0/0.25$ CO release.

$X_C = 0.25$ and $X_C = 1$ conversion degree. This implies that gaseous CO_2 during gasification exerts an instantaneous effect over the configuration of the sample surface that causes a change either in the configuration, volatilization or inactivation of ash components immediately after changing the atmosphere from Ar to CO_2.

Fig. 5(b) shows the CO release during the determination of stable complexes for the unconverted char ($X_C = 0$) as well as $X_C = 0.25$ and $X_C = 1$ conversion degree. Similar to the CO_2 signal (see Fig. 5(a)), the intensity of CO decreases with increasing carbon conversion degree. However, the course of the CO signal is similar to the signals during determination of total and stable surface complexes (see Fig. 4). The high intensity at $X_C = 0$ conversion degree may be the result from CO forming reactions of carbon and silica which is present in the quartz wool layers surrounding the sample [52]. The CO signal at $X_C = 1$ conversion degree was the same one as used as base line and subtracted from the CO signals obtained in all the other TPD experiments, as it was assumed to be a systematic error for the determination of RSA. Thus, no CO signal for $X_C = 1$ is depicted.

For the calculation of RSA by difference of total and stable surface complexes, the effects of ash decomposition and silica-carbon reactions need to be taken into account. Part 2 of the paper will address this issue in detail.

5. Summary

Based on the carbon conversion mechanism proposed by Lizzio et al. [9] for the gasification of carbon with CO_2, a method for the determination of active sites during gasification of biomass char is presented. The investigations were conducted with beech wood char that underwent secondary pyrolysis in a drop-tube reactor at 1600 °C in order to imitate entrained-flow gasification conditions. This secondary char was partially gasified in CO_2 followed by a temperature-programmed desorption in order to determine total and stable surface complexes as a function of carbon conversion degree. The experiments were conducted in a temperature controlled quartz glass reactor at atmospheric pressure coupled with a mass spectrometer for the detection of desorbed gas species spectra.

The observed desorption spectra of CO and CO_2 during TPD cannot completely be explained by the underlying mechanistic model. Discrepancies arise from the following findings:

- CO_2 release around $T = 430$ °C implies higher amount of stable complexes than total complexes.
- CO signals of total and stable complexes do not reach baseline line level in the isothermal part of the TPD at $T = 900$ °C.

The interpretation of the obtained TPD spectra as function of carbon conversion degree are summarized as follows:

- Similar CO_2 signals for total and stable surface complexes are observed for all carbon conversion degrees. This may be explained by either:
  - o the amount of stable C-O does not depend on gasification progress, i.e. is similar for all carbon conversion degrees.
  - o observed CO_2 is released only by ash decomposed during TPD.
- Increased release of CO during the determination of total and stable surface complexes at $X_C = 0.9$ may originate from:
  - o Enhanced formation of oxygenated surface complexes at $Xc = 0.9$.
  - o Decomposition of potassium carbonates at temperatures higher than $T = 700$ °C mainly yielding CO.

The measured CO_2 and CO concentration spectra indicate that the gas species released during TPD may originate from desorption of surface complexes as well as from decomposition of ash components. Both signals must be differentiated in order to determine reactive surface area (RSA) as a function of carbon conversion degree to be implemented in Eq. 1 describing the specific char conversion rate R_m.

Part 2 of the paper addresses the influence of inorganic matter on CO_2 and CO signals obtained from TPD. An activated carbon is impregnated with Ca and K being the main components of beech wood char. A direct relationship between specific conversion rate and the amount of reactive sites is presented.

Declaration of Competing Interest

The authors declare that they have no known competing financial interests or personal relationships that could have appeared to influence the work reported in this paper.

Acknowledgments

The authors gratefully acknowledge the financial support by the Helmholtz Association of German Research Centres (HGF) in the frame of the Helmholtz Virtual Institute for Gasification Technology – HVIGasTech (VH-VI-429) and the German Academic Exchange Service (DAAD) for funding the research visits of Prof. Rincón at KIT.

References

[1] Kolb T, Aigner M, Kneer R, Müller M, Weber R, Djordjevic N. Tackling the challenges in modelling entrained-flow gasification of low-grade feedstock. J. Energy Inst. 2016;89(4):485–503. https://doi.org/10.1016/j.joei.2015.07.007.

[2] Eberhard M, Santo U, Böning D, Schmid H, Michelfelder B, Zimmerlin B, et al. Der bioliq®-Flugstromvergaser - ein Baustein der Energiewende. Chem. Ing. Tech. 2018;90(1–2):85–98. https://doi.org/10.1002/cite.201700086.

[3] Di Blasi C. Combustion and gasification rates of lignocellulosic chars. Prog. Energy Combust. Sci. 2009;35(2):121–40. https://doi.org/10.1016/j.pecs.2008.08.001.

[4] Guizani C, Jeguirim M, Gadiou R, Escudero Sanz FJ, Salvador S. Biomass char gasification by H_2O, CO_2 and their mixture: evolution of chemical, textural and structural properties of the chars. Energy 2016;112:133–45. https://doi.org/10.1016/j.energy.2016.06.065.

[5] Laurendeau NM. Heterogeneous kinetics of coal char gasification and combustion. Prog. Energy Combust. Sci. 1978;4(4):221–70. https://doi.org/10.1016/0360-1285(78)90008-4.

[6] Radović LR, Walker PL, Jenkins RG. Importance of carbon active sites in the gasification of coal chars. Fuel 1983;62(7):849–56. https://doi.org/10.1016/0016-2361(83)90041-8.

[7] Wölki M. Über die wahre Reaktionsgeschwindigkeit der Vergasung von Biomassepyrolysat mit Kohlendioxid und Wasserdampf. Kassel: Kassel Univ. Press; 2005.

[8] Klose W, Wölki M. On the intrinsic reaction rate of biomass char gasification with carbon dioxide and steam. Fuel 2005;84(7):885–92. https://doi.org/10.1016/j.fuel.2004.11.016.

[9] Lizzio AA, Jiang H, Radovic LR. On the kinetics of carbon (Char) gasification: reconciling models with experiments. Carbon 1990;28(1):7–19. https://doi.org/10.1016/0008-6223(90)90087-F.

[10] Bhatia SK, Perlmutter DD. A random pore model for fluid-solid reactions: I. Isothermal, kinetic control. AIChE J. 1980;26(3):379–86. https://doi.org/10.1002/aic.690260308.

[11] Gómez-Barea A, Leckner B. Modelling of biomass gasification in fluidized bed. Prog. Energy Combust. Sci. 2010;36(4):444–509. https://doi.org/10.1016/j.pecs.2009.12.002.

[12] Duman G, Uddin MA, Yanik J. The effect of char properties on gasification reactivity. Fuel Process. Technol. 2014;118:75–81. https://doi.org/10.1016/j.fuproc.2013.08.006.

[13] Rincón S, Gómez A, Klose W. Gasificación de biomasa residual de procesamiento agroindustrial. kassel university press GmbH; 2011.

[14] Wang G, Zhang J, Shao J, Liu Z, Wang H, Li X, et al. Experimental and modeling studies on CO 2 gasification of biomass chars. Energy 2016;114:143–54. https://doi.org/10.1016/j.energy.2016.08.002.

[15] Struis RPWJ, von Scala C, Stucki S, Prins R. Gasification reactivity of charcoal with CO_2 Part I: Conversion and structural phenomena. Chem. Eng. Sci. 2002;57(17):3581–92. https://doi.org/10.1016/S0009-2509(02)00254-3.

[16] Zhang Y, Ashizawa M, Kajitani S, Miura K. Proposal of a semi-empirical kinetic model to reconcile with gasification reactivity profiles of biomass chars. Fuel 2008;87(4):475–81. https://doi.org/10.1016/j.fuel.2007.04.026.

[17] Fatehi H, Bai X-S. Structural evolution of biomass char and its effect on the gasification rate. Appl. Energy 2017;185:998–1006. https://doi.org/10.1016/j.apenergy.2015.12.093.

[18] Singer SL, Ghoniem AF. An adaptive random pore model for multimodal pore structure evolution with application to char gasification. Energy Fuels 2011;25(4):1423–37. https://doi.org/10.1021/ef101532u.

[19] Gómez A, Klose W, Rincón S. Thermogravimetrische Untersuchungen zur Entwicklung des Porensystems bei der einstufigen Teilvergasung von Biomasse. Chem. Ing. Tech. 2008;80(5):631–9. https://doi.org/10.1002/cite.200700159.

[20] Fu P, Hu S, Xiang J, Yi W, Bai X, Sun L, et al. Evolution of char structure during steam gasification of the chars produced from rapid pyrolysis of rice husk. Bioresour. Technol. 2012;114:691–7. https://doi.org/10.1016/j.biortech.2012.03.072.

[21] Bouraoui Z, Jeguirim M, Guizani C, Limousy L, Dupont C, Gadiou R. Thermogravimetric study on the influence of structural, textural and chemical properties of biomass chars on CO_2 gasification reactivity. Energy 2015;88:703–10. https://doi.org/10.1016/j.energy.2015.05.100.

[22] Laine NR, Vastola FJ, Walker Jr PL. The importance of active surface area in the carbon-oxygen reaction. J. Phys. Chem. 1963;67(10):2030–4.

[23] Radovic LR. Importance of carbon active sites in coal char gasification—8 years later. Carbon 1991;29(6):809–11. https://doi.org/10.1016/0008-6223(91)90020-J.

[24] Brunauer S, Emmett PH, Teller E. Adsorption of gases in multimolecular layers. J. Am. Chem. Soc. 1938;60(2):309–19.

[25] Dubinin MM, Zaverina ED, Radushkevich LV. Sorption and structure of active carbons. I. Adsorption of organic vapors. Zh. Fiz. Khim. 1947;21(3):151–62.

[26] Figueiredo JL, Pereira MFR, Freitas MMA, Órfão JJM. Modification of the surface chemistry of activated carbons. Carbon 1999;37(9):1379–89. https://doi.org/10.1016/S0008-6223(98)00333-9.

[27] Figueiredo JL, Pereira MFR, Freitas MMA, Órfão JJM. Characterization of active sites on carbon catalysts. Ind. Eng. Chem. Res. 2007;46(12):4110–5. https://doi.org/10.1021/ie061071v.

[28] Figueiredo JL, Pereira MFR. The role of surface chemistry in catalysis with carbons. Catal. Today 2010;150(1–2):2–7. https://doi.org/10.1016/j.cattod.2009.04.010.

[29] Szymanski GS, Karpinski Z, Biniak S, Swiatkowski A. The effect of the gradual thermal decomposition of surface oxygen species on the chemical and catalytic properties of oxidized activated carbon. Carbon 2002;40(14):2627–39. https://doi.org/10.1016/S0008-6223(02)00188-4.

[30] Tremblay G, Vastola FJ, Walker PL. Thermal desorption analysis of oxygen surface complexes on carbon. Carbon 1978;16(1):35–9. https://doi.org/10.1016/0008-6223(78)90113-6.

[31] Walker PL, Taylor RL, Ranish JM. An update on the carbon-oxygen reaction. Carbon 1991;29(3):411–21. https://doi.org/10.1016/0008-6223(91)90210-A.

[32] Freund H. Gasification of carbon by CO_2: a transient kinetics experiment. Fuel 1986;65(1):63–6. https://doi.org/10.1016/0016-2361(86)90143-2.

[33] Kyotani T, Yamada H, Yamashita H, Tomita A, Radovic LR. Use of transient kinetics and temperature-programmed desorption to predict carbon/char reactivity: the case of copper-catalyzed gasification of coal char in oxygen. Energy Fuels 1992;6(6):865–7.

[34] Radovic LR, Jiang H, Lizzio AA. A transient kinetics study of char gasification in carbon dioxide and oxygen. Energy Fuels 1991;5(1):68–74.

[35] Kapteijn F, Meijer R, Moulijn JA, Cazorla-Amóros D. On why do different carbons show different gasification rates: a transient isotopic CO_2 gasification study. Carbon 1994;32(7):1223–31. https://doi.org/10.1016/0008-6223(94)90106-6.

[36] Zhu ZB, Furusawa T, Adschiri T, Nozaki T. Characterization of coal char reactivity by the number of active sites during CO2 gasification. Prepr. Pap., Am. Chem. Soc., Div. Fuel Chem; (United States) 1989;34:1.

[37] Lizzio A, Radovic LR. Temperature-programmed desorption studies of coal char gasification. Prepr. Pap. (Am. Chem. Soc., Div. Fuel Chem.) 1989:102–11.

[38] Laine NR, Vastola FJ, Walker Jr PL. The role of the surface complex in the carbon-oxygen reaction. Proceedings of the Fifth Carbon Conference. 1963. p. 211.

[39] Kyotani T, Karasawa S, Tomita A. A TPD study of coal chars in relation to the catalysis of mineral matter. Fuel 1986;65(10):1466–9. https://doi.org/10.1016/0016-2361(86)90125-0.

[40] Ranish JM, Walker PLJR. Desorption turnover numbers for the carbon-oxygen reaction. Prepr. Pap., Am. Chem. Soc., Div. Fuel Chem; (United States) 1987;32:4.

[41] Zoulalian A, Bounaceur R, Dufour A. Kinetic modelling of char gasification by accounting for the evolution of the reactive surface area. Chem. Eng. Sci. 2015;138:281–90. https://doi.org/10.1016/j.ces.2015.07.035.

[42] Morgano MT, Leibold H, Richter F, Seifert H. Screw pyrolysis with integrated sequential hot gas filtration. J. Anal. Appl. Pyrol. 2015;113:216–24. https://doi.org/10.1016/j.jaap.2014.12.019.

[43] Stoesser P, Ruf J, Gupta R, Djordjevic N, Kolb T. Contribution to the understanding of secondary pyrolysis of biomass-based slurry under entrained-flow gasification conditions. Energy Fuels 2016;30(8):6448–57. https://doi.org/10.1021/acs.energyfuels.6b00935.

[44] Stoesser P, Schneider C, Kreitzberg T, Kneer R, Kolb T. On the influence of different experimental systems on measured heterogeneous gasification kinetics. Appl. Energy 2018;211:582–9. https://doi.org/10.1016/j.apenergy.2017.11.037.

[45] Kienitz H, Aulinger F. Massenspektrometrie: VerlagChemie 1968.

[46] Linstrom PJ, Mallard WG. NIST Chemistry WebBook, NIST Standard Reference Database Number 69. Gaithersburg MD: National Institute of Standards and Technology.

[47] Mu J, Perlmutter DD. Thermal decomposition of carbonates, carboxylates, oxalates, acetates, formates, and hydroxides. Thermochim Acta 1981;49(2):207–18. https://doi.org/10.1016/0040-6031(81)80175-X.

[48] McKee DW. Catalytic effects of alkaline earth carbonates in the carbon-carbon dioxide reaction. Fuel 1980;59(5):308–14. https://doi.org/10.1016/0016-2361(80)90215-X.

[49] Rodriguez-Navarro C, Ruiz-Agudo E, Luque A, Rodriguez-Navarro AB, Ortega-Huertas M. Thermal decomposition of calcite: mechanisms of formation and textural evolution of CaO nanocrystals. Am. Mineral. 2009;94(4):578–93. https://doi.org/10.2138/am.2009.3021.

[50] Dollimore D, Tong P, Alexander KS. The kinetic interpretation of the decomposition of calcium carbonate by use of relationships other than the Arrhenius equation. Thermochim Acta 1996;282–283:13–27. https://doi.org/10.1016/0040-6031(95)02810-2.

[51] Linares-Solano A, Almela-Alarcón M, Lecea CS-Md. CO2 chemisorption to characterize calcium catalysts in carbon gasification reactions. J. Catal. 1990;125(2):401–10. https://doi.org/10.1016/0021-9517(90)90313-9.

[52] Hüttinger KJ, Nill JS. A method for the determination of active sites and true activation energies in carbon gasification: (II) Experimental results. Carbon 1990;28(4):457–65. https://doi.org/10.1016/0008-6223(90)90039-2.

[53] Henderson JB, Tant MR. A study of the kinetics of high-temperature carbon-silica reactions in an ablative polymer composite. Polym. Compos. 1983;4(4):233–7. https://doi.org/10.1002/pc.750040408.

[54] Kopyscinski J, Rahman M, Gupta R, Mims CA, Hill JM. K_2CO_3 catalyzed CO_2 gasification of ash-free coal. Interactions of the catalyst with carbon in N_2 and CO_2 atmosphere. Fuel 2014;117:1181–9. https://doi.org/10.1016/j.fuel.2013.07.030.

[55] Lehman RL, Gentry JS, Glumac NG. Thermal stability of potassium carbonate near its melting point. Thermochim Acta 1998;316(1):1–9. https://doi.org/10.1016/S0040-6031(98)00289-5.

[56] Cazorla-Amoros D, Linares-Solano A, Salinas-Martinez de Lecea C, Yamashita H, Kyotani T, Tomita A, et al. XAFS and thermogravimetry study of the sintering of calcium supported on carbon. Energy Fuels 1993;7(1):139–45.

Glossary

Symbol: Description (Unit)
a_{28}*:* Relative intensity (–)
C_{Cf}*:* Concentration of active sites of fixed carbon (mol/g)

d: Diameter (m)
$\frac{dX}{dt}$: Conversion rate (1/s)
$I_{m/z}$: Ion current of a mass-to-charge ratio (A)
k: Specific conversion rate constant (g/(mol s))
M: Molar mass (g/mol)
m: Mass (g)
$\dot{n}$: Molar flow (mol/s)
p_{total}: Total system pressure (bar)
R_{m}: Specific conversion rate. 1/s
S: Calibration sensitivity (A/bar)
T: Temperature (K)
t: Time (S)
X: Conversion degree (-)
y: Volume fraction (vol.-%)

Subscripts

28: Mass-to-charge ratio 28
C: Carbon
f: Fixed carbon
i: Gas species
in: Inlet gas flow
m/z: Mass-to-charge ratio
out: Outlet gas flow

Abbreviations

ad: Air dried
Ar: Argon
ASA: Active surface area
BET: Brunauer-Emmett-Teller
Ca: Calcium
daf: Dry ash free
DR: Dubinin-Radushkevich
EFG: Entrained-flow gasification
MRPM: Modified random pore model
RPM: Random pore model
RSA: Reactive surface area
TK: Transient kinetics
TPD: Temperature-programmed desorption
TSA: Total surface area
TSC: Total surface complexes
UASA: Unoccupied active surface area
vol.: Volume
wt.: Weight